

Received May 31, 2021, accepted July 15, 2021, date of publication August 3, 2021, date of current version August 24, 2021.

Digital Object Identifier 10.1109/ACCESS.2021.3102423

BS-HTIS: Buffer Sizing for Heterogeneous Traffic and Integrated System

HUAIFENG SHI^{1,2}, CHENGSHENG PAN^{1,2}, AND YINGZHI WANG²

¹School of Automation, Nanjing University of Science and Technology, Nanjing 210094, China

²School of Electronic and Information Engineering, Nanjing University of Information Science and Technology, Nanjing 210044, China

Corresponding authors: Huaifeng Shi (shihuaifeng314@126.com) and Chengsheng Pan (pancs@sohu.com)

This work was supported by the National Natural Science Foundation of China under Grant 61801073, Grant 61722105, and Grant 61931004.

ABSTRACT Buffer sizing for switching and routing devices is of significance for guaranteeing the Quality of Service (QoS) of critical services on the Internet of Things (IoT), continuously evolving scheduling mechanisms and complex traffic characteristics pose new challenges for the traditional method of static buffer sizing based on rule-of-thumb. In this paper, the scope of buffer sizing is extended from a basic scheduling system under homogeneous arrival traffic input to an integrated scheduling system under heterogeneous arrival traffic input which is more ubiquitous. In this context, Voices, videos and other heterogeneous data in the IoT are categorized into short-range-dependent (SRD) and long-range-dependent (LRD) traffic, and the integrated scheduling system is decomposed into single-server-single-queue (SSSQ) systems by not only decoupling the complex dependencies among heterogeneous traffic inputs but also taking the impact of SRD and LRD traffic burstiness on the buffer sizing into account. On this basis, expressions for the relation between the minimum buffer size and the maximum overflow probability are presented. The numerical analysis results and simulation analysis results reveal that the average arrival rate, traffic burst level and scheduling priority are positively correlated with the required buffer size, and once the overflow probability is set, the minimum buffer size can be determined correspondingly. The achievements of this paper will provide theoretical guidance for IoT manufacturers and technicians to set buffers more reasonably and use resources more efficiently.

INDEX TERMS SRD traffic, LRD traffic, integrated scheduling, buffer sizing.

I. INTRODUCTION

The Internet of Things (IoT), as the envisaged future internet, has recently become a hot research topic for both industry and academia recently [1]. It is anticipated that there will be 24.6 billion IoT connected devices by 2025, and global monthly mobile data traffic will reach 164 exabytes [2]. Billions of digital devices and other physical objects, generate tremendous amounts of voices, images, files, videos and other heterogeneous service data.

The diversification of services leads to a surge in IoT traffic, which easily causes network congestion, increases the forwarding delay, and even packet loss. As a result, the service quality deteriorates or the service becomes unavailable completely. At the same time, users have

The associate editor coordinating the review of this manuscript and approving it for publication was Yuan Tian¹.

increasing requirements for high-quality, high-speed, and low-latency network services. Traditionally, the most intuitive way to solve network congestion and ensure the quality of service (QoS) is to increase the bandwidth of the network, but considering the associated operation and maintenance costs, this is not realistic.

Buffer sizing is an important part of network configuration and plays a critical role in guaranteeing the QoS of heterogeneous traffic [3]. At present, the configuration of buffer size in engineering is mainly based on rule-of-thumb, lacking theoretical performance guarantee, which results in low resource utilization. In fact, buffer sizing has always been a hot research topic, and many scholars have performed many significant studies [4]–[7]. These studies include two broad categories of analytical buffer sizing methods. The first one involves the use of stochastic service theory, also known as queuing theory [8]. That is, given an input traffic

model and service model, the queuing theory is used to analyze the queue length distribution, and then the appropriate buffer size is obtained. This method can be roughly divided into two directions: short-range-dependent (SRD) and long-range-dependent (LRD) queuing analysis. The latter is based on the TCP model [9]–[11]. The representative conclusions include rule-of-thumb, small buffer rule, tiny buffer rule and packet drop rate-based buffer rule.

Generally, the setting of buffer size is usually determined by two elements in theory: the traffic arrival process and the system service process. However, differentiated burst levels of arrival traffic and the integrated scheduling mechanism of service system pose new challenges for the traditional method of static buffer sizing.

For one thing, different types of traffic always have differentiated burst levels, the stronger the traffic burst, the larger the buffer increment. Specifically, many high-quality measurement studies have proven that the traffic of real-world network exhibits heterogeneous characteristics and can be divided into two distinct categories, namely SRD and LRD traffic [12], [13]. Furthermore, there are significant differences in the buffer size requirements for heterogeneous traffic. When SRD traffic enters the buffer for queuing, the overflow probability has a negative exponential relationship with the buffer size, that is, a small buffer can meet the packet loss rate requirement of SRD traffic; However, when LRD traffic is used as the input, the overflow probability has the property of a power function, and only a large buffer can meet the packet loss rate requirement of LRD traffic. Therefore, SRD and LRD traffic cannot be aggregated together to calculate the required buffer, because the aggregation of traffic will lead to the burst of traffic being absorbed, affecting the accuracy of buffer sizing.

For another thing, the integrated scheduling mechanism of the five service system determines the service priority and service rate of each queue, and profoundly affects the queue length and buffer size. Specifically, traffic scheduling realizes that switches and routers in the IoT select a queue to be forwarded from one or more queues. Common traffic scheduling methods include priority queuing (PQ), generalized processor sharing (GPS), round robin (RR), and their variants [14]–[16]. Due to the diversity of traffic in the IoT, a basic scheduling algorithm can no longer meet the requirements of bandwidth sharing for heterogeneous traffic, and integrated scheduling mechanisms combining different basic scheduling schemes, such as PQ+GPS, PQ+WRR or other variants [17], [18], have attracted significant research interest and have also been deployed on many IoT devices such as the Huawei CE12800 series and H3C MSR 5600 series. Therefore, an integrated scheduling algorithm is more conducive to guaranteeing the QoS of heterogeneous traffic. However, compared with a basic scheduling algorithm, an integrated scheduling mechanism is more complex with respect to the allocation of service rates on the output link, which makes it face more difficulty analyzing the needs of each queue for buffer sizing.

In this paper, we integrate the traffic arrival process and system service process in a queuing system organically and explore the optimal buffer size for heterogeneous traffic aggregation nodes based on the above conditions. Specifically, in terms of the traffic arrival process, we model heterogeneous traffic via Markov modulated Poisson processes (MMPP) for SRD traffic and fractional Brownian motion (fBm) processes for LRD traffic [19]. Regarding the traffic arrival process, we use the common PQ-GPS integrated scheduling mechanism [20], so that some traffic flows are served with strictly high priority, and other traffic flows are handled by the conventional GPS scheduling mechanism. Our main contributions are summarized as follows:

(1) Based on the traffic arrival process and the system service process, the mathematical expression of the relationship between the maximum overflow probability and the minimum buffer size is derived, which innovates the traditional rule-of-thumb dominated buffer sizing method in IoT switching and routing devices, and provides theoretical guidance for IoT manufacturers and technicians to set buffer more reasonably and use resources more efficiently.

(2) From homogeneous arrival traffic to heterogeneous arrival traffic, from basic scheduling systems to integrated scheduling systems, a more ubiquitous application context is considered. In this context, calculating the minimum buffer size of the integrated system in an overall way will ignore the impact of heterogeneous traffic with different burst levels on the buffer sizing and obtain loose minimum buffer size boundary. To this end, heterogeneous arrival traffic is clustered into SRD traffic and LRD traffic, and the integrated system is decomposed into single-server-single-queue (SSSQ) systems, making it possible to obtain a more tight buffer boundary for each flow in this complex context.

(3) By using numerical analysis method and simulation analysis method, the accuracy of the expression of the relationship between the maximum overflow probability and the minimum buffer size is verified by setting various parameters in four typical scenarios.

The remainder of the paper is organized as follows. Section II summarizes the related traffic models. Section III presents the expressions for calculating the minimum buffer size and overflow probability of each individual flow. Section IV verifies the proposed approach by a numerical calculation and a network simulation. Section V presents the conclusion drawn from this research.

II. PREREQUISITES

As mentioned in Section I, heterogeneous traffic is usually divided into two distinct categories, namely SRD traffic and LRD traffic. Moreover, SRD traffic and LRD traffic have different burst levels and have distinct effects on buffer sizing. Consequently, to calculate the buffer size required under different burst levels numerically and accurately, we introduce an SRD traffic model and an LRD traffic model in this Section.

A. SRD TRAFFIC MODEL

SRD traffic often represents delay-sensitive services such as voice and command services. Most SRD traffic models, e.g., fluid-flow model, MMPP model, packet-train model and batch arrival Markov process are based on a Markov process. In this article, an MMPP model is used as the SRD traffic model.

An MMPP model is a kind of stochastic double Poisson process whose arrival rate is modulated by a multistate irreducible Markov process, and MMPP model has been proven to be quite accurate in voice traffic modeling. A two-state MMPP is adopted in this paper to characterize high-priority traffic.

Specifically, a two-state MMPP is uniquely determined by an infinitesimal generator matrix used to modulate the Markov chain and intensity vector of a Poisson process, which are denoted as Ω and Λ , respectively.

$$\Omega = \begin{bmatrix} -\gamma_1 & \gamma_1 \\ \gamma_2 & -\gamma_2 \end{bmatrix} \text{ and } \Lambda = \begin{bmatrix} \eta_1 & 0 \\ 0 & \eta_2 \end{bmatrix} \quad (1)$$

where γ_i ($i = 1, 2$) is the transition rate from state i to another state, and η_i ($i = 1, 2$) is the traffic arrival rate at state i .

For an MMPP traffic flow, the cumulative amount of traffic arrived up to time t , $A_m(t)$ can be expressed as

$$A_m(t) = \lambda_m t + Z_m(t) \quad (2)$$

where $\lambda_m = (\eta_1 \gamma_2 + \eta_2 \gamma_1) / (\gamma_1 + \gamma_2)$ is the mean arrival rate of $A_m(t)$, and $E(Z_m(t)) = 0$. The variance of $A_m(t)$ is given by

$$v_m(t) = \left(\frac{\eta_1 \gamma_2 + \eta_2 \gamma_1}{\gamma_1 + \gamma_2} \right)^2 t^2 + \frac{2(\eta_1 - \eta_2)^2 \gamma_1 \gamma_2}{(\gamma_1 + \gamma_2)^3} t - \frac{2(\eta_1 - \eta_2)^2 \gamma_1 \gamma_2}{(\gamma_1 + \gamma_2)^4} (1 - e^{-(\gamma_1 + \gamma_2)t}) \quad (3)$$

B. LRD TRAFFIC MODEL

LRD traffic often represents bandwidth-sensitive services such as files or videos. Many traffic models have been built to characterize LRD traffic, such as fractal Brown motion (fBm) model, heavy-tailed on/off model, M/G/ ∞ queuing model. Among them, the fBm model is considered an effective method for LRD traffic modeling in terms of temporal and spatial complexity. Thus, we use an fBm model as the LRD traffic model in this paper.

For an fBm traffic flow, the cumulative amount of traffic arrived up to time t , $A_f(t)$ can be expressed as

$$A_f(t) = \lambda_f t + Z_f(t) \quad (4)$$

where $Z_f(t) = \sqrt{a_f \lambda_f} Z_f(t)$, λ_f is the mean arrival rate, a_f is the variance coefficient, and $Z_f(t)$ is a standard fBm with variance $\bar{v}_f(t) = t^{2H_f}$, in which $H_f \in (0.5, 1)$ is the Hurst parameter. The variance function of $A_f(t)$ can be given as follows

$$v_f(t) = a_f \lambda_f \bar{v}_f(t) = a_f \lambda_f t^{2H_f} \quad (5)$$

III. BUFFER SIZING

In Section 2, we introduced the SRD traffic model and the LRD traffic model, which enable us to obtain the first element required for determining the buffer size of each flow of the traffic arrival process. Furthermore, we need to decompose the integrated scheduling system to obtain the second element that determines the buffer size of each flow of the system service process.

In this section, we design a system model using the Diff-Serv framework. Based on this framework, we combine the expression of the total queue length distribution and extended empty buffer approximation (EBA) theory to decompose the PQ-GPS integrated scheduling system and obtain the minimum buffer size corresponding to the maximum overflow probability for each flow, which can provide theoretical buffer sizing guidance for IoT devices manufacturers and technicians.

A. SYSTEM MODEL

The DiffServ framework is defined by the Internet Engineering Task Force (IETF) to provide differentiated QoS for heterogeneous traffic. In DiffServ, expedited forwarding (EF) represents accelerated forwarding behavior, which is usually applied to delay sensitive traffic. Assured forwarding (AF) involves ensuring forwarding behavior, which is usually applied to bandwidth sensitive traffic. Best effort (BE) stands for best effort forwarding behavior, which is applied to best effort forwarding traffic that does not require strict QoS guarantees, and focuses only on accessibility.

In order to ensure that traffic with different sensitivities can obtain services with different priority levels, we design an integrated scheduling system model based on the DiffServ framework, as shown in Figure 1.

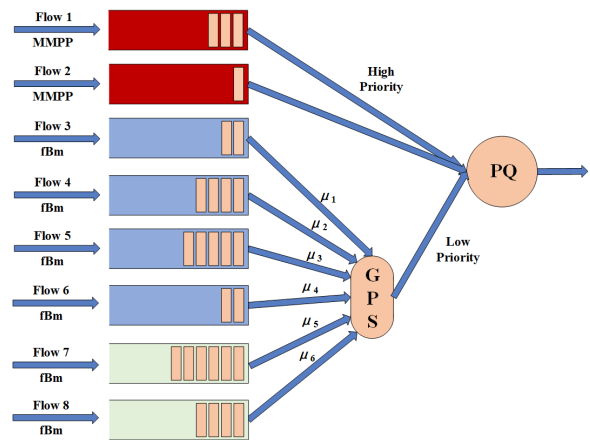


FIGURE 1. PQ-GPS scheduling system model.

According to the flow classification rules of integrated scheduling, we divide the input traffic into eight flows in the system model. Among them, Flow 1 and Flow 2 represent EF services and are depicted by MMPP models. Flow 3, Flow 4, Flow 5 and Flow 6 represent AF services and are depicted by

fBm models. Flow 7 and Flow 8 represent BE services and are also depicted by fBm models.

In addition, we use a PQ-GPS integrated scheduling mechanism to schedule eight heterogeneous traffic. Among them, Flow 1 and Flow 2 have strictly high priority and are used to represent voice, command and other delay-sensitive services. The other flows have low priority levels, and each flow is assigned a weight to guarantee a minimum service rate and handled by GPS mechanism. This property provides forwarding guarantees for individual traffic flows and prevents them from experiencing service starvation. Finally, all eight flows are scheduled in turn through the PQ mechanism.

B. TOTAL QUEUE LENGTH DISTRIBUTION

Notably, fBm is a Gaussian process, and an MMPP can also be approximated as a Gaussian process when time tends to infinity [11]. According to the large deviation principle (LDP) method, the variance $v(t)$ of Gaussian traffic $A(t)$ for queuing satisfies $\lim_{x \rightarrow \infty} v(t)/t^\alpha = 0, \exists \alpha < 2$. Then, the upper bound and lower bound of the total queue length distribution can be derived as follows:

$$\text{Upper bound: } P(Q > x) \leq \exp\left(-\frac{1}{2}\Theta(t_x)\right) \quad (6)$$

$$\text{Lower bound: } P(Q > x) \geq \frac{\exp\left(-\frac{1}{2}\Theta(t_x)\right)}{\sqrt{2\pi(1 + \sqrt{\Theta(t_x)})^2}} \quad (7)$$

where $\Theta(t_x)$ is the determinative function of queue length distribution, which is given by

$$\Theta(t) = \frac{(-x + (C - \lambda)t)^2}{v(t)} \quad (8)$$

where x is the queue length, C is the service rate, λ is the arrival rate, and $v(t)$ is the variance of the arrival traffic.

The parameter t_x minimizes $\Theta(t)$, i.e., $t_x = \arg \min_t \Theta(t)$. By differentiating this equation and solving $\Theta'(t) = 0$, we obtain the required value t_x that minimizes $\Theta(t)$.

It can be seen from Equation (6) and Equation (7) that the difference between the two bounds of the total queue length distribution is the parameter $\exp(-\Theta(t_x)/2)$. Here, we can further take the geometric average of the upper and lower bounds [11], therefore, the total queue length distribution can be given by the following equation:

$$P(Q > x) \approx \frac{\exp\left(-\frac{1}{2}\Theta(t_x)\right)}{\sqrt[4]{2\pi(1 + \sqrt{\Theta(t_x)})^2}} \quad (9)$$

Specifically, for the PQ-GPS system model in this paper, we concretize the determinative function to the following equation:

$$\Theta(t) = \frac{\left(-x + (C - \sum_{m=1}^p \lambda_m - \sum_{f=p+1}^n \lambda_f)t\right)^2}{\sum_{i=1}^p v_m + \sum_{f=p+1}^n v_f} \quad (10)$$

where n is the total number of flows in the integrated scheduling system, p is the number of high priority flows, and $n - p$ is

the number of low priority flows. λ_m is given by Equation (2), λ_f is given by Equation (4), $v_m(t)$ is given by Equation (3), and $v_f(t)$ is given by Equation (5).

C. PQ-GPS SCHEDULING SYSTEM DECOMPOSITION

As mentioned above, to obtain more accurate buffer sizes for individual traffic flows, we need to decompose the complex PQ-GPS system into a series of individual SSSQ systems, and the key is to obtain the service rate of each SSSQ.

Specifically, the service rate of SSSQ $_m$ is denoted by $c_m (m \in [1, p])$. As MMPP flows have high priority, they are processed as if the GPS subsystem does not exist. As a result, by allocating the total link capacity to the MMPP traffic flows one by one, it is easy to determine that the service rate of SSSQ $_m$ is $c_m = C$. Moreover, only when all the traffic in SSSQ $_1$ is served, can the traffic in SSSQ $_2$ be served, and so on for SSSQ $_m$.

Based on this principle, the total queue length distribution of the PQ-GPS system is approximately the queue length distribution of the GPS subsystem. If we take $\Theta(t)$ as the determinative function of the PQ-GPS system, and $\Phi(s)$ as the determinative function of GPS subsystem, then we have $\min_t \Theta(t) = \min_s \Phi(s)$, i.e., $\Theta(t_x) = \Phi(s_x)$. By solving this equation, we can finally obtain the service rate of the GPS subsystem, which is denoted as c_{GPS} .

The service rate of SSSQ $_f$ is, denoted by $c_f (f \in [p + 1, n])$. However, the fBm traffic flows in the GPS subsystem share links and are interdependent; thus, it is not easy to calculate c_f . Fortunately, EBA shows that the total queue length distribution of the whole heterogeneous traffic is similar to that of the low priority traffic.

Proposition 1: The service capacity of the GPS system, c_{GPS} , can be approximately calculated by solving the following equation:

$$\Theta(t_x) = \Phi(s_x) \quad (11)$$

where $t_x = \arg \min_t \Theta(t)$, and $s_x = \arg \min_s \Phi(s)$.

$$\Phi(s) = \frac{\left(-x + (c_{GPS} - \sum_{f=p+1}^n \lambda_f)s\right)^2}{\sum_{f=p+1}^n v_f} \quad (12)$$

The required value s_x that minimizes $\Phi(s)$ can be obtained by differentiating this equation and solving $\Phi'(s) = 0$.

Furthermore, we need to discuss how to derive the expression of c_f from the expression for c_{GPS} in the GPS subsystem. Specifically, we assume that the guaranteed service rate received by fBm $_f (f \in [p + 1, n])$ can be given by $\mu_f c_{GPS}$. If $\mu_f c_{GPS} - \lambda_f \geq 0$, it denotes the excess service received by fBm $_f$. Otherwise, fBm $_f$ needs additional service, and thus, $|\mu_f c_{GPS} - \lambda_f|$ denotes the service deficit. That is, we can solve the service capacity problem in two situations.

Situation 1: fBm $_i (i \in [p + 1, n])$ is the guaranteed excess service while fBm $_j (j \in [p + 1, n], j \neq i)$ represents that the fBm requires additional service. Consequently, fBm $_j$ cannot be served in a timely manner and becomes the dominant contributor of the total GPS subsystem queue, which means

that the total queue length distribution of the GPS subsystem can be used to approximate that of fBm_j .

Proposition 2: The service capacity of $SSSQ_j$, c_j , can be approximately calculated by solving the following equation:

$$\Phi(s_x) = \Gamma(u_x) \tag{13}$$

where $s_x = \arg \min_s \Phi(s)$, and $u_x = \arg \min_u \Gamma(u)$.

$$\Gamma(u) = \frac{(-x + (\sum c_j - \sum \lambda_j)u)^2}{\sum a_j \lambda_j u^{2H_j}} \tag{14}$$

The required value μ_x that minimizes $\Gamma(u)$ can be obtained by differentiating this equation and solving $\Gamma'(u) = 0$.

According to the joint Equations (10), (11), (12), (13) and (14), we know that, when the Hurst parameters of heterogeneous fBm traffic are not exactly the same, it is difficult to obtain a closed expression for c_j . However, if all of the fBm traffic flows have the same Hurst parameter H , then we can obtain a closed expression. In this case, we have

$$u_x = \frac{Hx}{(\sum c_j - \sum \lambda_j)(H - 1)} \tag{15}$$

$$\Gamma(u_x) = \frac{\left(\frac{x}{H-1}\right)^2}{\sum a_j \lambda_j \left(\frac{Hx}{(\sum c_j - \sum \lambda_j)(H-1)}\right)^{2H}} \tag{16}$$

$$\sum c_j = \sum \lambda_j + \left(c_{GPS} - \sum \lambda_k\right) \left(\frac{\sum a_j \lambda_j}{\sum a_k \lambda_k}\right)^{\frac{1}{2H}} \tag{17}$$

where $k \in [p + 1, n]$.

$$c_i = \mu_i c_{GPS} \tag{18}$$

Situation II: $fBm_i (i \in [p + 1, n])$, $fBm_j (j \in [p + 1, n], j \neq i)$ are guaranteed excess services. However, due to the bursty nature of fBm flow, there is a certain time interval in which some flows have temporary excess service, while other flows require additional service. In this case, the service capacity c_i can be calculated as follows:

$$c_i = \mu_i c_{GPS} + \left(\sum \mu_j c_{GPS} - \sum \lambda_j\right) \left(\frac{a_i \lambda_i}{\sum a_k \lambda_k}\right)^{\frac{1}{2H}} \tag{19}$$

where $k \in [p + 1, n]$.

D. OPTIMAL BUFFER SIZE BASED ON QUEUE LENGTH

After obtaining the service capability $c_k (k \in [1, n])$ of a single SSSQ system, the buffer size analysis of the complex PQ-GPS system can be transformed into the analysis of these equivalent SSSQ systems whose analysis process is simpler and whose analysis results are more accurate.

Specifically, given the service capacity c_k of $SSSQ_k$ and the equivalence relationship between the k^{th} traffic flow and $SSSQ_k$, the queue length distribution, $P(Q_k > x)$, based on Equations (9) and (10) is obtained by setting $n = 1$ and $C = c_k$ as follows:

$$P(Q_k > x) \approx \frac{\exp\left(-\frac{1}{2}\Theta_k(t_x)\right)}{\sqrt{2\pi}\left(1 + \sqrt{\Theta_k(t_x)}\right)^2} \tag{20}$$

where

$$\Theta_k(t) = \frac{(-x + (c_k - \lambda_k)t)^2}{v_k(t)} \tag{21}$$

On the one hand, if the maximum probability of buffer overflow in the k^{th} traffic flow is Δ_m , based on Equations (3), (20) and (21), the minimum buffer size b_m^* of MMPP SRD traffic can be obtained.

$$P(Q_k > x) = \Delta_m \tag{22}$$

where $k \in [1, p]$.

$$b_m^* = \arg \max(\Delta_m) \tag{23}$$

On the other hand, if the maximum probability of buffer overflow in k^{th} traffic flow is Δ_m , based on Equations (5), (17), (18) or (19), (20) and (21), the minimum buffer size b_f^* of fBm LRD traffic can be obtained.

$$P(Q_k > x) = \Delta_f \tag{24}$$

where $k \in [p + 1, n]$.

$$b_f^* = \arg \max(\Delta_f) \tag{25}$$

IV. MODEL VALIDATION

In this section, we verify the model through four scenarios, and each scenario uses two methods, one that employs Python for numerical analysis and another that utilizes NS3 for simulation analysis. Without loss of generality, for the PQ-GPS integrated scheduling system, we set the number of EF service queues represented by the MMPP model to 1, the number of AF service queues represented by the fBm model to 2, and the number of BE service queues represented by the fBm model to 1.

A. SCENARIO I

In this scenario, we set four traffic flows, MMPP1, fBm2, fBm3, and fBm4, which correspond to the EF service, AF1 service, AF2 service, and BE service, respectively. The specific parameters for these traffic flows are shown in Table 1, which lists the parameters used to explore buffer sizing under Situation I introduced in Section III-C.

TABLE 1. Parameter settings in scenario I.

Queue	Parameters				
MMPP1 (EF)	$\eta_1=50$	$\gamma_1=0.2$	$\eta_2=30$	$\gamma_2=0.8$	C=200
fBm2 (AF1)	$a_2=1.0$	$H_2=0.8$	$\lambda_2=40$	$\mu_2=0.3$	
fBm3 (AF2)	$a_3=1.0$	$H_3=0.8$	$\lambda_3=40$	$\mu_3=0.3$	
fBm4 (BE)	$a_4=1.0$	$H_4=0.8$	$\lambda_4=90$	$\mu_4=0.4$	

Table 2 and Figure 2 illustrate the minimum buffer sizes of heterogeneous traffic under different maximum overflow probability requirements.

Table 2 and Figure 2 reveal that, once the maximum overflow probability of a traffic flow is determined, the minimum

TABLE 2. Buffer sizing analysis results in scenario I.

Queue	Minimum buffer size	Maximum overflow probability					
		10^{-6}	10^{-5}	10^{-4}	10^{-3}	10^{-2}	10^{-1}
MMPP1	Analysis	0	0	0	0	0	0
	Simulation	0	0	0	0	0	0
fBm2	Analysis	119	109	53	20	3	0
	Simulation	120	110	50	20	5	0
fBm3	Analysis	119	109	53	20	4	0
	Simulation	120	110	50	20	5	0
fBm4	Analysis	1411	856	459	201	59	6
	Simulation	1400	850	450	200	50	0

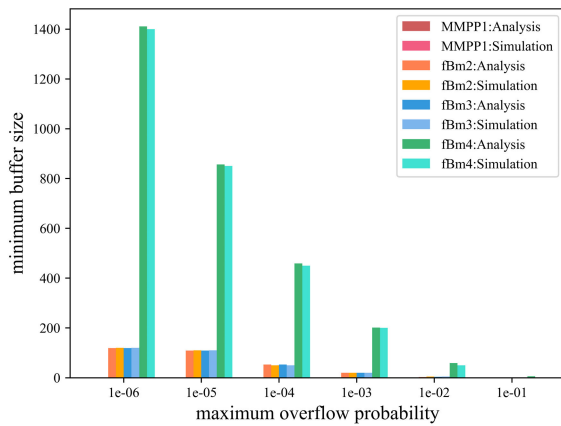


FIGURE 2. Buffer sizing analysis results in scenario I.

buffer size is determined accordingly. Moreover, the smaller the maximum overflow probability is required, the larger the minimum buffer size is required.

Specifically, the minimum buffer size under any maximum overflow probability for traffic flow MMPP1 is zero in Table 2 and Figure 2. The reason for this is that compared with the service capacity ($C = 200$) of the PQ-GPS integrated scheduling system, the average arrival rate of traffic flow MMPP1 is relatively small ($\lambda_1 = 46$). At the same time, traffic flow MMPP1 is a strictly high-priority flow, and fBm2, fBm3 and fBm4 are regarded as nonexistent traffic flows, thus, MMPP1 can get timely service.

In addition, for low-priority traffic flows in the GPS subsystem, under different maximum overflow probabilities, the minimum buffer size of fBm2 and fBm3 is the same, but the minimum buffer size of fBm4 is much larger than that of fBm2 and fBm3. The reason for this is that, fBm2 and fBm3 are guaranteed excess service and they have the same average arrival rate, burst level and service rate, which means the traffic arrival process and system service process of fBm2 and fBm3 are consistent, so the requirements on buffer sizing for fBm2 and fBm3 are the same. However, quite different from the previous two, fBm4 requires additional

service, which means that traffic in fBm4 flow cannot be processed in a timely manner, so the requirement on buffer sizing for fBm4 is much larger.

B. SCENARIO II

In this scenario, we set four traffic flows, MMPP1, fBm2, fBm3, and fBm4, which correspond to the EF service, AF1 service, AF2 service, and BE service, respectively. The specific parameters for these traffic flows are shown in Table 3, which lists the parameters used to explore buffer sizing under Situation I introduced in Section III-C. Different from Table 1, we change some parameters of MMPP1, fBm2 and fBm4 to obtain some comparative conclusions.

TABLE 3. Parameter settings in scenario II.

Queue	Parameters				
MMPP1 (EF)	$\eta_1=80$	$\gamma_1=0.02$	$\eta_2=80$	$\gamma_2=0.8$	C=200
fBm2 (AF1)	$a_2=1.0$	$H_2=0.9$	$\lambda_2=45$	$\mu_2=0.3$	
fBm3 (AF2)	$a_3=1.0$	$H_3=0.8$	$\lambda_3=45$	$\mu_3=0.3$	
fBm4 (BE)	$a_4=0.5$	$H_4=0.7$	$\lambda_4=90$	$\mu_4=0.4$	

Table 4 and Figure 3 illustrate the minimum buffer sizes of heterogeneous traffic under different maximum overflow probability requirements.

TABLE 4. Buffer sizing analysis results in scenario II.

Queue	Minimum buffer size	Maximum overflow probability					
		10^{-6}	10^{-5}	10^{-4}	10^{-3}	10^{-2}	10^{-1}
MMPP1	Analysis	0	0	0	0	0	0
	Simulation	0	0	0	0	0	0
fBm2	Analysis	1787	656	188	36	5	0
	Simulation	1800	650	200	50	0	0
fBm3	Analysis	160	127	83	22	5	0
	Simulation	160	130	90	25	0	0
fBm4	Analysis	377	249	143	63	13	0
	Simulation	400	250	150	70	15	0

According to the comparative analysis between Table 2 and 4, as well as between Figure 2 and Figure 3, we can draw the following conclusions.

Although we change the transition rate of MMPP1 and increase its burst level, the conclusion is the same as Scenario I. since MMPP1 has a relatively small average arrival rate as compared to the service rate of the integrated scheduling system and it is served with strict high-priority, no traffic of MMPP1 need to be buffered.

In addition, for low-priority traffic flows in the GPS subsystem, we set the burst parameter of fBm2 as $H = 0.9$ and that of fBm3 as $H = 0.8$, and ensure the consistency of other parameters of the two. The result is that under the same maximum overflow probability, the minimum buffer size of fBm2 is much larger than that of fBm3. The reason for this

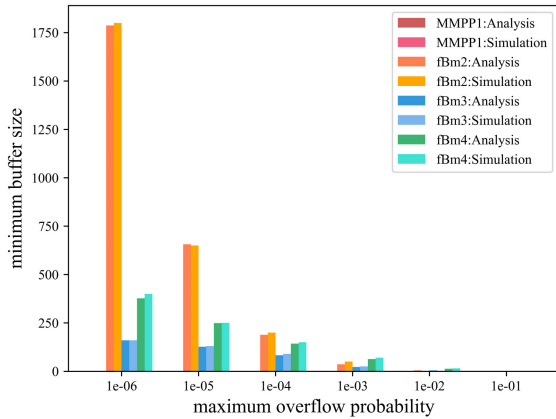


FIGURE 3. Buffer sizing analysis results in scenario II.

is that, different types of services always have differentiated burst levels, the stronger the LRD traffic burst, the larger the buffer increment. Moreover, this conclusion is also applicable to fBm4. After we weaken the burstiness of fBm4, the minimum buffer size is significantly reduced.

C. SCENARIO III

In this scenario, we set four traffic flows, MMPP1, fBm2, fBm3, and fBm4, which correspond to the EF service, AF1 service, AF2 service, and BE service, respectively. The specific parameters for these traffic flows are shown in Table 5, which lists the parameters used to explore buffer sizing under Situation II introduced in Section III-C.

TABLE 5. Parameter settings in scenario III.

Queue	Parameters				C=200
MMPP1 (EF)	$\eta_1=160$	$\gamma_1=0.8$	$\eta_2=160$	$\gamma_2=0.2$	
fBm2 (AF1)	$a_2=0.5$	$H_2=0.8$	$\lambda_2=65$	$\mu_2=0.4$	
fBm3 (AF2)	$a_3=0.5$	$H_3=0.8$	$\lambda_3=55$	$\mu_3=0.3$	
fBm4 (BE)	$a_4=1.0$	$H_4=0.8$	$\lambda_4=55$	$\mu_4=0.3$	

Table 6 and Figure 4 illustrates the minimum buffer size of heterogeneous traffic under different maximum overflow probability requirements.

Table 6 and Figure 4 reveals that, when the average arrival rate of MMPP1 is relatively high and fBm2, fBm3, fBm4 are all guaranteed excess services, fBm4 is no longer the main contributor to the queue length of the integrated scheduling system.

Specifically, in Table 6 and Figure 4, if the maximum overflow probability is less than 10^{-4} , the minimum buffer size of MMPP1s should be greater than 0. And the reason is, compared with the service capacity ($C = 200$) of the PQ-GPS integrated scheduling system, the average arrival rate of traffic flow MMPP1 is relatively high ($\lambda_1 = 160$). However, since the traffic flow MMPP1 is a strictly high priority flow and can get timely service, the minimum buffer

TABLE 6. Buffer sizing analysis results in scenario III.

Queue	Minimum buffer size	Maximum overflow probability					
		10^{-6}	10^{-5}	10^{-4}	10^{-3}	10^{-2}	10^{-1}
MMPP1	Analysis	19	9	1	0	0	0
	Simulation	20	10	0	0	0	0
fBm2	Analysis	93	81	72	26	1	0
	Simulation	100	90	80	30	5	0
fBm3	Analysis	413	250	134	59	26	2
	Simulation	450	250	150	60	30	0
fBm4	Analysis	369	223	120	34	15	1
	Simulation	400	250	120	50	20	0

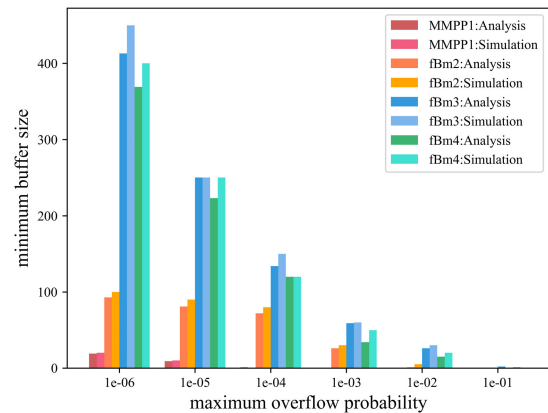


FIGURE 4. Buffer sizing analysis results in scenario III.

size are much less than those of fBm2, fBm3 and fBm4, although its average arrival rate is much larger than those of fBm2, fBm3 and fBm4.

In addition, for low-priority traffic flows in the GPS sub-system, We set the $c_i - \lambda_i$ of fBm2, fBm3 and fBm4 to be greater than 0, so they can all get excess service. The result is that under the same maximum overflow probability, the minimum buffer size of fBm3 and fBm4 is similar, but the minimum buffer size for fBm2 is much smaller. The reason for this is that, although fBm2, fBm3 and fBm4 are all guaranteed excess services, the excess services of fBm3 and fBm4 are the same and the burst level is similar, so the minimum buffer size required is basically the same. However, the relative excess services of fBm2 are larger than those of fBm3 and fBm4, so the minimum buffer size required is much smaller.

D. SCENARIO IV

In this scenario, we set four traffic flows, MMPP1, fBm2, fBm3, and fBm4, which correspond to the EF service, AF1 service, AF2 service, and BE service, respectively. The specific parameters for these traffic flows are shown in Table 7, which lists the parameters used to explore buffer sizing under Situation I introduced in Section III-C.

TABLE 7. The parameter settings in scenario IV.

Queue	Parameters				C=1000
MMPP1 (EF)	$\eta_1=900$	$\gamma_1=0.02$	$\eta_2=900$	$\gamma_2=0.01$	
fBm2 (AF1)	$a_2=0.5$	$H_2=0.8$	$\lambda_2=620$	$\mu_2=0.7$	
fBm3 (AF2)	$a_3=0.5$	$H_3=0.7$	$\lambda_3=180$	$\mu_3=0.2$	
fBm4 (BE)	$a_4=1.0$	$H_4=0.6$	$\lambda_4=150$	$\mu_4=0.1$	

Table 8 and Figure 5 illustrates the minimum buffer size of heterogeneous traffic under different maximum overflow probability requirements.

TABLE 8. Buffer sizing analysis results in scenario IV.

Queue	Minimum buffer size	Maximum overflow probability					
		10^{-6}	10^{-5}	10^{-4}	10^{-3}	10^{-2}	10^{-1}
MMPP1	Analysis	47	32	19	3	0	0
	Simulation	50	35	20	5	0	0
fBm2	Analysis	124	71	35	4	0	0
	Simulation	125	70	35	5	0	0
fBm3	Analysis	46	33	21	12	5	1
	Simulation	50	35	20	10	5	0
fBm4	Analysis	159	124	90	60	33	10
	Simulation	160	125	90	60	30	10

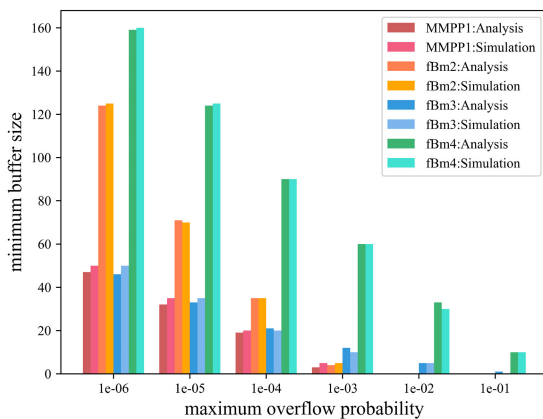


FIGURE 5. Buffer sizing analysis results in scenario IV.

Table 8 and Figure 5 reveals that, in the case that the service capacity of the PQ-GPS integrated scheduling system is significantly improved, consistent with the analysis conclusion of the first three scenarios, we still need the buffer sizing to queue the incoming traffic.

V. CONCLUSION

The rapid development of the IoT has brought many new services, some of which bring SRD traffic and some of which bring LRD traffic. When these heterogeneous traffic flows are

scheduled in switches or routers, the impact of heterogeneous traffic with different burst levels on the buffer sizing pose new challenges for designing the buffer sizes. To solve this problem, we cluster heterogeneous traffic in the IoT into MMPP SRD traffic and fBm LRD traffic, and decompose the integrated PQ-GPS scheduling system into SSSQ systems, thereby we derive expressions for calculating the minimum buffer size and maximum overflow probability of individual traffic flow based on EBA and LDP theory, and obtain the relationship between the minimum buffer size and maximum overflow probability for each flow. The results of numerical analysis and simulation analysis show that no matter how the service capacity is increased, the system’s demand for buffer sizing will not change, and the results of this paper will provide theoretical guidance for the development of IoT devices.

REFERENCES

- [1] K. Shafique, B. A. Khawaja, F. Sabir, S. Qazi, and M. Mustaqim, “Internet of Things (IoT) for next-generation smart systems: A review of current challenges, future trends and prospects for emerging 5G-IoT scenarios,” *IEEE Access*, vol. 8, pp. 23022–23040, Jan. 2020.
- [2] *Ericsson Mobility Report*, Ericsson, Stockholm, Sweden, 2020.
- [3] A. Showail, K. Jamshaid, and B. Shihada, “Buffer sizing in wireless networks: Challenges, solutions, and opportunities,” *IEEE Commun. Mag.*, vol. 54, no. 4, pp. 130–137, Apr. 2016.
- [4] A. Dhamdhere and C. Dovrolis, “Open issues in router buffer sizing,” *ACM SIGCOMM Comput. Commun. Rev.*, vol. 36, no. 1, pp. 87–92, Jan. 2006.
- [5] M. Enachescu, Y. Ganjali, A. Goel, N. McKeown, and T. Roughgarden, “Routers with very small buffers,” in *Proc. 25th IEEE Int. Conf. Comput. Commun. (INFOCOM)*, Apr. 2006, pp. 1–11.
- [6] N. Bouacida and B. Shihada, “Practical and dynamic buffer sizing using LearnQueue,” *IEEE Trans. Mobile Comput.*, vol. 18, no. 8, pp. 1885–1897, Aug. 2019.
- [7] R. G. Garroppo, S. Giordano, S. Lucetti, and F. Russo, “Comparison of LRD and SRD traffic models for the performance evaluation of finite buffer systems,” in *Proc. IEEE Int. Conf. Commun. Conf. Rec. (ICC)*, Helsinki, Finland, Jun. 2001, pp. 2681–2686.
- [8] L. Janowski and Z. Papir, “The influence of an SRD structure of LRD traffic on a drop probability,” *Syst. Sci.*, vol. 32, no. 3, pp. 89–96, Jan. 2006.
- [9] J. Semke, J. Mahdavi, and M. Mathis, “Automatic TCP buffer tuning,” *ACM SIGCOMM Comput. Commun. Rev.*, vol. 28, no. 4, pp. 315–323, Oct. 1998.
- [10] L. Xu, K. Xu, T. Li, K. Zheng, M. Shen, X. Du, and X. Du, “ABQ: Active buffer queueing in datacenters,” *IEEE Netw.*, vol. 34, no. 2, pp. 232–237, Mar. 2020.
- [11] X. Jin and G. Min, “Performance modelling of hybrid PQ-GPS systems under long-range dependent network traffic,” *IEEE Commun. Lett.*, vol. 11, no. 5, pp. 446–448, May 2007.
- [12] S. A. Stoev, G. Michailidis, and M. S. Taqqu, “Estimating heavy-tail exponents through max self-similarity,” *IEEE Trans. Inf. Theory*, vol. 57, no. 3, pp. 1615–1636, Mar. 2011.
- [13] N. Likhanov, B. Tsybakov, and N. D. Georganas, “Analysis of an ATM buffer with self-similar (‘fractal’) input traffic,” in *Proc. IEEE INFOCOM*, Boston, MA, USA, Apr. 1995, pp. 985–992.
- [14] N. McKeown, “The iSLIP scheduling algorithm for input-queued switches,” *IEEE/ACM Trans. Netw.*, vol. 7, no. 2, pp. 188–201, Apr. 1999.
- [15] M. Katevenis, S. Sidiropoulos, and C. Courcoubetis, “Weighted round-robin cell multiplexing in a general-purpose ATM switch chip,” *IEEE J. Sel. Areas Commun.*, vol. 9, no. 8, pp. 1265–1279, Oct. 1991.
- [16] H. Shimonishi, M. Yoshida, R. Fan, and H. Suzuki, “An improvement of weighted round Robin cell scheduling in ATM networks,” in *Proc. IEEE Global Telecommun. Conf. Conf. Rec. (GLOBECOM)*, Phoenix, AZ, USA, Nov. 1997, pp. 1119–1123.
- [17] J. Mao, W. M. Moh, and B. Wei, “PQWRR scheduling algorithm in supporting of DiffServ,” in *Proc. IEEE Int. Conf. Commun. Conf. Rec. (ICC)*, Helsinki, Finland, 2001.

- [18] J. Zheng, L. Yang, C. Pan, and H. Shi, "MQSD: A scheduling mechanism of mixed queue in the integrated intelligent network," in *Proc. J. Phys., Conf.*, Mar. 2021, vol. 1848, no. 1, Art. no. 012143.
- [19] H. Shi, C. Pan, L. Yang, D. Wei, and Y.-Q. Shi, "End-to-end latency evaluation of the Sat5G network based on stochastic network calculus," *Comput., Mater. Continua*, vol. 65, no. 2, pp. 1335–1348, 2020.
- [20] X. Jin and G. Min, "Modelling and analysis of an integrated scheduling scheme with heterogeneous LRD and SRD traffic," *IEEE Trans. Wireless Commun.*, vol. 12, no. 6, pp. 2598–2607, Jun. 2013.



HUAIFENG SHI was born in 1989. He received the B.E. and M.E. degrees from Nanjing University of Science and Technology (NUST), Nanjing, Jiangsu, China, in 2007 and 2011, respectively, where he is currently pursuing the Ph.D. degree. He was a Lecturer with Dalian University, in 2019. He is currently working as a Lecturer with Nanjing University of Information Science and Technology. His main research interests include space-ground integrated network technology and heterogeneous link aggregation methods in wireless networks.



CHENGSHENG PAN was born in 1962. He received the B.S. and M.S. degrees from Nanjing University of Science and Technology (NUST), in 1987, and the Ph.D. degree from Northeastern University, in 2001. From 1988 to 1989, he was a Co-Researcher with the Institute of Mathematics, Chinese Academy of Sciences. Since 1989, he has been an Assistant Professor with Shenyang Ligong University. He is currently a Professor with Nanjing University of Information Science and Technology and a part-time Ph.D. Tutor with Nanjing University of Science and Technology. He is the author of three books and more than 150 articles. His research interests include intelligent network traffic theory and key technologies.



YINGZHI WANG was born in 1994. He received the B.S. degree in communication engineering from Zhengzhou University, Zhengzhou, China, in 2017, and the M.S. degree in electronics and information engineering from Nanjing University of Information Science and Technology, Nanjing, China, in 2020, where he is currently pursuing the Ph.D. degree in information and communication engineering.

...